5th International Conference on Electrical and Computer Engineering
ICECE 2008, 20-22 December 2008, Dhaka, Bangladesh

Voltage Mode Control of Single Phase Boost Inverter

Ainul Anam Shahjamal Khan

Department of Electrical and Electronic Engineering,
Chittagong University of Engineering and Technology,
Chittagong-4349, Bangladesh
E-mail: khanshahjamal@yahoo.com

Kazi Mujibur Rahman

Department of Electrical and Electronic Engineering,
Bangladesh University of Engineering and Technology,
Dhaka, Bangladesh
E-mail: kmr@eee.buet.ac.bd

Abstract – Boost inverter is able to generate an ac voltage whose peak value can be larger or smaller than the dc input voltage in a single stage. The boost inverter consists of two individual boost dc-dc converters. Each of the boost dc-dc converters has to be controlled in variable operating point condition. This paper proposes two voltage mode controllers. First one is conventional feedback controller based on small signal model. Second one is a simplified voltage mode controller based on Feedforward Pulse Width Modulation (FF-PWM) and simple voltage feedback loop to control the output voltage of the boost inverter. The second controller gave better result. The controller also ensures output voltage to meet IEEE Std 519 voltage harmonic limits. Unlike most previously proposed controllers, the proposed method is based only on output voltage feedback, making unnecessary the inductor current measurement. The control method is verified by means of simulations.

I. Introduction

Boost DC-AC inverter [l] is a novel converter, whose main advantage is to achieve an output voltage higher or lower than the input one. Other advantages are the quality of output voltage sine wave and reduced number of switches i.e. only four switches required.

This property is not found in the traditional full bridge inverter, which produces an instantaneous ac output voltage always lower than the input dc voltage. The power stage of boost inverter consists of two current bi-directional dc-dc boost converters and the load is connected differentially across them as in Fig. 1. Each converter produce a dc-biased sinusoidal waveform as Fig. 2. The modulation of each converter is 180 degrees out of phase with respect to the other, which maximizes the voltage excursion across the load.

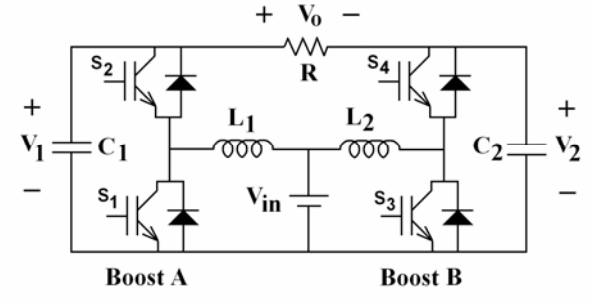

Fig. 1 The boost inverter.

The DC and small-signal performance of a boost DC to AC converter can be determined by substituting the circuit by PWM switch model [2,3] and analyzing the resultant linear circuit. The converter can be modeled using the models of the current-bidirectional switch based Phase-leg averaging technique [4].

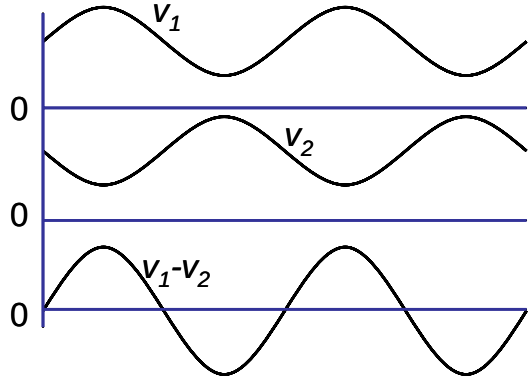

Fig. 2 Typical waveforms of the basic approach to achieve dc–ac conversion, with boost characteristics.

Several control techniques have been proposed to control the individual boost of the boost inverter [1, 5-7]. The sliding mode controller [1] involves complex theory, variable switching frequency and also involves current mode control in addition to voltage mode. The effect of supply voltage variation on output voltage is not reported. A controller based on Energy Shaping theory [5] is proposed which is a complex one. An adaptive control [6] designed for the boost inverter in order to cope with RL load. This involves very complex non-linear control theory. A double-loop regulation scheme [7] is a very robust controller including compensations in order to cope with the boost variable operation point condition. But it has also current loop and circuit complexity. So a simplified controller with only voltage mode control and meet the IEEE Standard for THD of the output voltage can be a simplified option to control the boost inverter.

This paper proposes two voltage mode control strategy. First one is based on traditional design of feedback loops which is based on frequency domain analysis after linearization. A linearized model of the boost inverter is determined and control to output transfer function is obtained from it. Second method is based on FF-PWM [8] which has inherent capability of reducing input source disturbances, improved steady-state and dynamic responses. A simplified outer voltage feedback loop is found to be sufficient to get good regulation of output

voltage under different load and source variations. The main advantage of this method over current mode control is its simplicity.

II. Modelling of the Boost Inverter and Conventional Control Approach

The boost inverter is modeled in [9] using PWM switch model described in [2]. Here we used a simplified method to model it. The main step is to replace converter phase legs with voltage and current sources [4]. The waveforms of voltage and current sources are identical to the switch waveforms of the converter. Then the converter waveforms are averaged over one switching period to remove switching harmonics. Any nonlinear element in the phase leg's average model is perturbed and linearized leading to small-signal ac model [10].

The boost inverter is usually classified as current bidirectional converters because they share the same switching cells that are current bidirectional. The switching network averaging is performed on a phase-leg basis [4]. After the phase-leg averaging, the average model of any current-bidirectional converter can be easily obtained by connecting the averaged phase legs.

In the current-bidirectional switch based converters, a generic switching unit, called a phase leg, can be identified, as shown in Fig. 3.

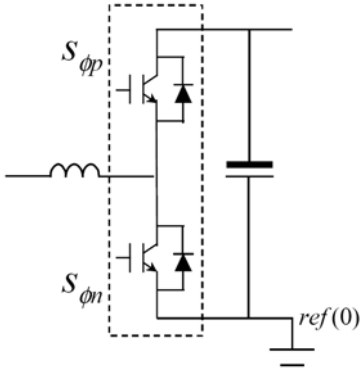

Fig. 3 Generic phase leg in current-bidirectional converters.

The phase leg is composed of two switching cells, and has a voltage source (or a capacitor) on one side and a current source (or an inductor) on the other. These features make the phase leg a generic switching unit. The phase leg can be represented by a single-pole, double-throw switch, as shown in Fig. 4.

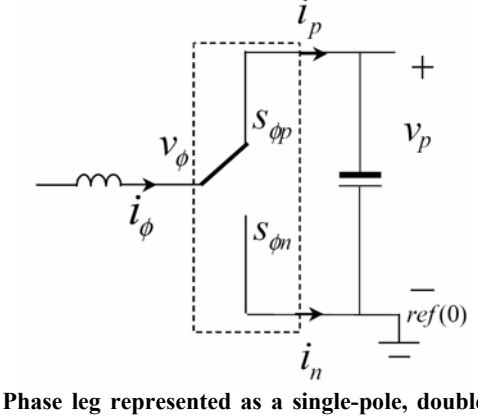

Fig. 4 Phase leg represented as a single-pole, double-throw switch.

A. DC model of PWM switch using Phase-Leg Average Model

Let us first assume that the duty ratio is fixed at D_ϕ and it is the duty cycle of the top switch $S_{\phi p}$. The PWM of the phase leg in DC is shown in Fig. 5, where T is the switching period. The corresponding voltage and current waveforms are also shown in Fig. 5.

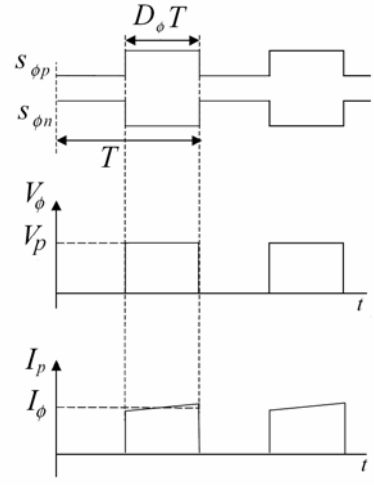

Fig. 5 PWM of Phase leg in DC and corresponding current and voltage waveforms

Based on the waveforms, the voltage and current relationships in average, assuming the current I_ϕ and the voltage V_p are continuous with small ripples:

$$V_\phi = D_\phi V_p \quad (1)$$

$$I_p = D_\phi I_\phi \quad (2)$$

The average DC model based on (1) and (2) of the phase leg is depicted in Fig. 6.

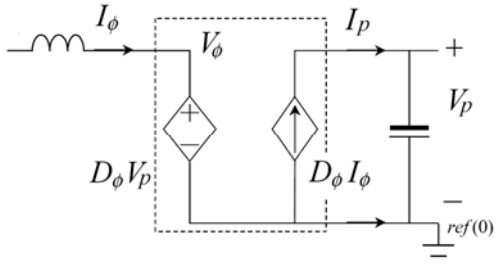

Fig. 6 Phase leg's average DC model.

B. Small signal model of PWM switch using Phase-Leg Average model

To construct a small-signal ac model at a quiescent operating point we assume that, duty cycle is perturbed around a quiescent value D_ϕ such that.

$$\langle d_\phi(t) \rangle = D_\phi + d_\phi(t) \quad (3)$$

where $d_\phi(t)$ is small ac variation. Using similar arguments we can write

$$\langle v_\phi(t) \rangle_{T_S} = V_\phi + v_\phi(t) \text{ etc.} \quad (4)$$

With the assumption that the ac variations are small in magnitude compared to the dc quiescent values, such as

$v_\phi(t) << V_\phi$. We will employ the basic approximation of removing the high-frequency switching ripple by averaging over one switching period

$$\langle x(t)\rangle_{T_S} = \frac{1}{T_S}\int_{t}^{t+T_S} x(\tau)d\tau \tag{5}$$

By averaging all signals over one switching period using equation (1)

$$\langle v_\phi(t)\rangle_{T_S} = \langle d_\phi(t)\rangle\langle v_p(t)\rangle_{T_S} \tag{6}$$

$$\Rightarrow V_\phi + v_\phi(t) = \underbrace{D_\phi V_p}_{DC\ terms} + \underbrace{d_\phi(t)V_p + D_\phi v_p(t)}_{1st\ order\ ac\ terms(linear)} + \underbrace{d_\phi(t)v_p(t)}_{2nd\ order\ ac\ terms(nonlinear)} \tag{7}$$

We can neglect the non-linear ac terms provided that the small signal assumption is satisfied, then each of the second order non-linear terms is much smaller in magnitude than on or more of the linear first-order terms [10]. The linearization step can be explained more analytically by taking the Taylor expansion of a nonlinear relation and retaining only constant and linear terms. The dc terms on the right hand side of the equation are equal to the dc terms on the left hand side. Then (7) becomes

$$v_\phi(t) = D_\phi v_p(t) + d_\phi(t)V_p \tag{8}$$

Using similar arguments

$$i_p(t) = D_\phi i_\phi(t) + d_\phi(t)I_\phi \tag{9}$$

For convenience we use $d_\phi(t) \Rightarrow d_\phi$, $v_\phi(t) \Rightarrow v_\phi$ etc.

Then equations (10) and (11) becomes

$$v_\phi = D_\phi v_p + d_\phi V_p \tag{10}$$

$$i_p = D_\phi i_\phi + d_\phi I_\phi \tag{11}$$

Equations (10) and (11) are small signal linearized equation that describes the phase-leg's average model in ac. The small signal model using equations (10) and (11) of the phase leg is depicted in Fig. 7.

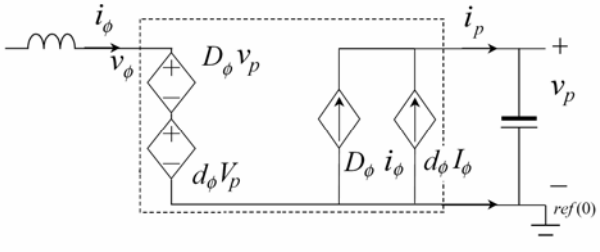

Fig. 7 Phase leg's average small signal ac model.

C. DC Analysis

Phase leg's average DC model in the boost inverter of Fig. 6 is substituted into the dc-ac boost inverter circuit of Fig. 1. The resulting circuit is shown in Fig. 8. In this circuit all inductances are shorted and capacitances are opened which is required for DC.

After analyzing the circuit of Fig. 8 we find the following relations:

$$V_1 = \frac{V_{in}}{(1-D)};\ V_2 = \frac{V_{in}}{D};\ V_o = \frac{V_{in}(2D-1)}{D(1-D)}$$

$$I_{L1} = \frac{V_{in}(2D-1)}{2RD(1-D)^2};\ I_{L2} = \frac{-V_{in}(2D-1)}{2RD^2(1-D)}$$

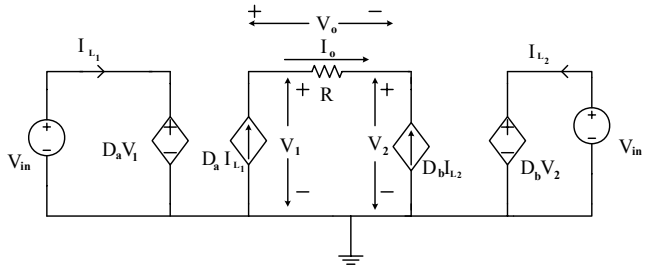

Fig. 8 DC model of the boost inverter.

D. Control to Output Transfer Function

In this case we are only considering the perturbations in the duty ratio. Here the input voltage source V_{in} is shorted to ground and the Phase leg's average small signal ac model of Fig. 7 is inserted in Fig. 1 as shown in Fig. 9.

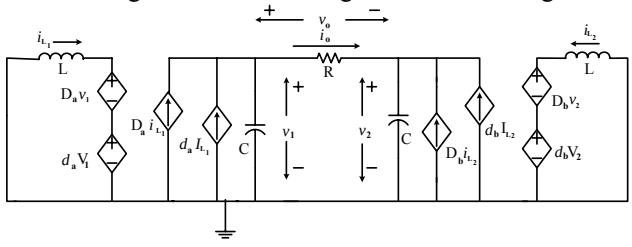

Fig. 9 Small signal ac model of the boost inverter

Here $d_b = d$, $d_a = -d$, $D_b = D$, $D_a = 1-D$

After analyzing the circuit of Fig. 9 we obtain the following control to output transfer function

$$\frac{v_o(s)}{d(s)} = -R\frac{Q_1s^3 + Q_2s^2 + Q_3s + Q_4}{T_1s^4 + T_2s^3 + T_3s^2 + T_4s + T_5} \tag{12}$$

Where, v_o = output voltage; d = variation of duty cycle around 0.5; R =load resistance

$Q_1 = (I_{L_1} + I_{L_2})CL^2$; $Q_2 = [(D-1)V_1 - DV_2]CL$;

$Q_3 = [I_{L_1}D^2 + I_{L_2}(D-1)^2]L$;

$Q_4 = [DV_1 - (D-1)V_2](D-1)D$;

$T_1 = RC^2L^2$; $T_2 = 2CL^2$; $T_3 = RCL(1-2D+2D^2)$;

$T_4 = L(1-2D+2D^2)$; $T_5 = R(D-1)^2D^2$

E. Conventional Control Using Small Signal Model

A conventional voltage mode controller is designed using the transfer function. We designed it taking the following parameters as shown in Fig. 10. $H = 1/36$, $V_M = 10$, $RC = 2.2736\times10^{-4}$, low pass filter cut off $f_{LP} = 700$, $k_p = 0.2$, $k_i = 50$. The capacitance, inductance and source voltage values of [1] are chosen. Capacitors 40uF each; Inductors 800uH each; Vin=100V. When the phase margin of the loop gain T is positive, then the feedback system is stable. Moreover increasing the phase margin causes the system transient response to be better behaved, with less overshoot and ringing [10]. The bode plot of T reveals that there is only one crossover frequency and phase margin of T is 113 degree

which is positive. So the feedback system is stable with good transient response.

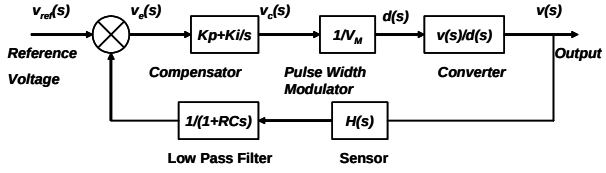

Fig. 10 Small signal block diagram of conventional voltage mode control.

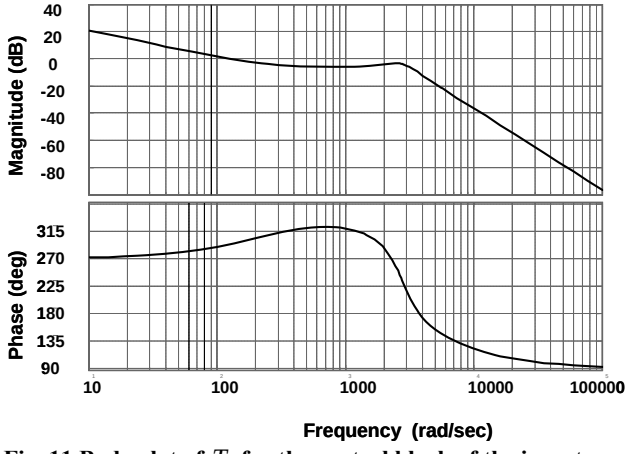

Fig. 11 Bode plot of T for the control block of the inverter.

F. Simulation Results

The inverter was simulated in ORCAD using the following parameters along with those mentioned in last section: S1,S2,S3,S4=> IRGBC40F; Diodes D1-D4=> MR2406F; Lock out time=2us; Switching frequency fc=5k; Nominal output voltage, Vomax=182.2 and frequency=50Hz and Nominal Load=30Ω. For load 30 Ω, THD=4.76% and Fourier component of fundamental voltage=182.2V. For load 60 Ω, THD=3.91% and fourier component of fundamental voltage=185.6V.

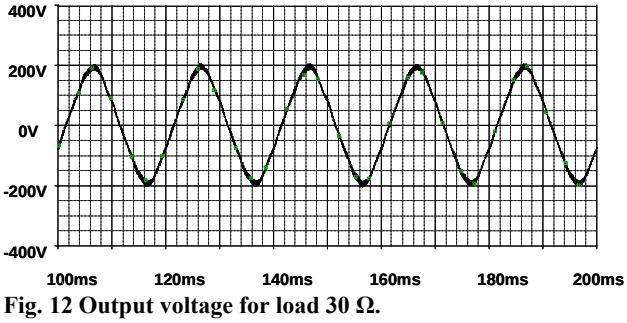

Fig. 12 Output voltage for load 30 Ω.

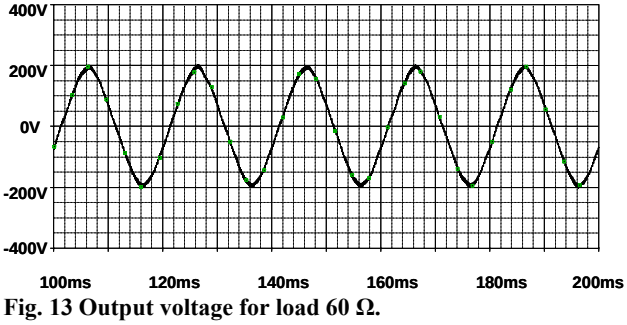

Fig. 13 Output voltage for load 60 Ω.

The controller works moderately well with resistive load keeping THD within IEEE Std 519 voltage harmonic limits. But it fails to regulate the output for inductive loads. In next section feedforward compensation technique is used to regulate the output voltage against source and inductive and resistive load variations.

III. Control of the Boost Inverter by FF-PWM with Simple Voltage Feedback Loop

For switching converters, feedforward compensation [8] is effective in reducing effects of source disturbances on converter outputs and improving steady-state and dynamic responses. The FF-PWM [8] yields good wide-range open loop line regulation and simplified design of an outer voltage feedback loop. A converter with FF-PWM behaves at low frequencies as a linear power amplifier with constant gain independent of operating conditions such that $V_o = Av_m$ where v_m is the modulating input, and A is a constant, independent of operating conditions. The saw-tooth carrier waveform of conventional PWM is periodic as in Fig. 14, it is sufficient to define the modulator during one switching period, say from 0 to T_s.

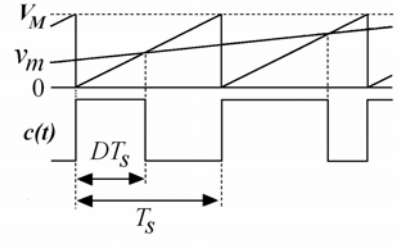

Fig. 14 Typical waveforms in the conventional PWM.

In this interval, the output logic-level function $c(t)$ is determined by

$$c(t) = 1, \quad \text{if} \quad g(t/T_s, v_m) > 0 \text{ and}$$
$$c(t) = 0, \quad \text{if} \quad g(t/T_s, v_m) \le 0, \quad 0 \le t \le T_s \qquad (13)$$
$$g(t/T_s, v_m) = v_m - V_M(t/T_s) \qquad (14)$$

Where, $g(t/T_s, v_m)$ is the modulator function. The output duty ratio D of the pulsating waveform $c(t)$ solves the equation

$$g(D, v_m) = 0 \qquad (15)$$

where $D \longrightarrow t/T_s$. In duty-ratio controlled switch-mode power converters operating in the continuous conduction mode, the output voltage V_o is a function of the input voltage V_g and the duty ratio D,

$$\frac{V_o}{V_g} = M(D) = \frac{P(D)}{Q(D)} \qquad (16)$$

The basics of FF-PWM are briefly described below for clarity. Detail analysis is presented in [8]. The first step in the synthesis of FF-PWM is to remove the assumption about the up-going saw-tooth carrier waveform and to allow feedforward inputs for the disturbance (independent source) that is desired to compensate. The converter is supplied from a single voltage source V_g. A modulator function, $g(t/T_s, V_g, v_m)$ is constructed so that the converter steady-state output V_o is independent of V_g

and directly proportional to the modulating control input v_m i.e.

$$V_o = Av_m \tag{17}$$

where A is a constant. If we combine the objective (17) and the conversion ratio (16), the duty ratio at the output of the FF-PWM must solve

$$\frac{V_o}{V_g} = \frac{P(D)}{Q(D)} \Rightarrow v_m Q(D) - \frac{1}{A} V_g P(D) = 0 \tag{18}$$

Equations (18) and (15) are similar equation with same variables. So equation (18) also gives a modulator function for the FF-PWM, if we let $D \longrightarrow t/T_s$.

So, a FF-PWM for any converter with specified $M(D)$ is defined by the modified modulator function

$$g_{TE}(t/T_s, V_g, v_m) = v_m Q(t/T_s) - \frac{1}{A} V_g P(t/T_s) \tag{19}$$

The subscript TE indicates the usual trailing-edge modulator. An equivalent leading-edge FF-PWM can be obtained simply by taking $D' = (1-D) \longrightarrow t/T_s$ in (18), which yields

$$g_{LE}(t/T_s, V_g, v_m) = v_m Q(1-t/T_s) - \frac{1}{A} V_g P(1-t/T_s) \tag{20}$$

In the modulator functions given by (19) or (20), there are terms of the form, $u(t)(t/T_s)^k$, where $u(t)$ is a linear combination of V_g and v_m . These terms can be implemented based on the use of integrators with reset.

For $k = 1$ we have,

$$u(t)\left(\frac{t}{T_s}\right) \approx \frac{1}{T_s}\int_0^t u(\tau)d\tau \tag{21}$$

The required building blocks include a voltage comparator, an integrator with reset, and a monostable pulse circuit (one-shot) with a short pulse output.

A voltage comparator outputs a logic high (‘‘1’’) if $v^+ > v^-$, and a logic low (‘‘0’’) if $v^+ \le v^-$, where v^+ and v^- are the voltages at the + and - the input of the comparator. An integrator with reset produces zero output $v_o = 0$ if the logic-level reset input R is high ($R = 1$), or the integral of the input v_i if $R = 0$. Assuming that R goes from 1 to 0 at $t = 0$, the output is given by

$$v_o = \frac{1}{T_i}\int_0^t v_i(\tau)d\tau \tag{22}$$

A constant-frequency clock generator CLK is required which outputs short pulses with period $T_s = T_i$ where T_i is the time-constant of the integrator. For the boost converter $P(D) = 1$ and $Q(D) = 1 - D$.

A leading-edge modulator function for the boost converter is

$$g_{LE}(t/T_s, V_g, v_m) = v_m \frac{t}{T_s} - \frac{1}{A} V_g \tag{23}$$

The implementation is shown in Fig. 15, with typical waveforms shown in Fig. 16.

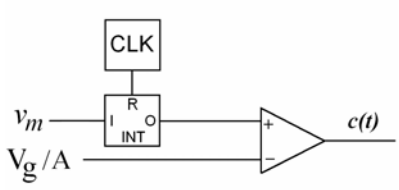

Fig. 15 Leading-edge FF-PWM for the boost converter.

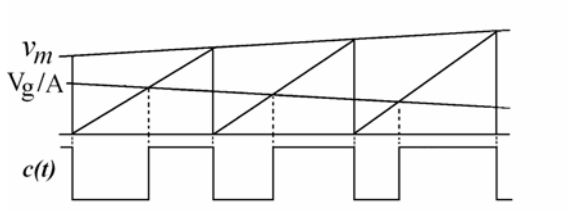

Fig. 16 Typical waveforms in the FF-PWM for the boost converter with leading-edge modulator.

The leading edge modulator is simpler than trailing edge modulator and in the leading-edge FF-PWM, the integrator time constant T_i does not have to match the switching period T_s [8]

A. Simplification of the Feedback Loop using FF-PWM

The FF-PWM results in a constant control-to-output gain. To regulate the output voltage, an outer voltage feedback loop is closed with fewer difficulties as shown in Fig. 17 Here we used two separate controllers for each of the individual dc-dc boost converter.

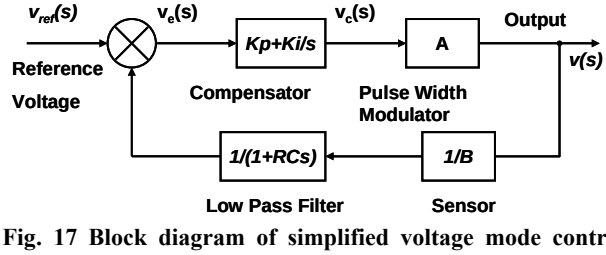

Fig. 17 Block diagram of simplified voltage mode control using FF-PWM.

We selected the same circuit component values [1] with $B = A$; $k_p = 0.3$, $k_i = 50$. The bode plot of T is shows is only one crossover frequency and phase margin of T is 107 degree which is positive. So the feedback system is stable with good transient response.

B. Simulation Results:

The inverter was simulated in ORCAD using the same parameters mentioned in last section II along with the following ones: Gain of feedforward pulse width modulator A=58.75; Sensor gain 1/B=1/58.75; Clock pulse =1us; Lock out time=2us; Switching frequency fc=5k; Nominal output voltage Vomax=185.8V frequency=50Hz and Nominal Load=30Ω. For load 30 Ω, THD=2.43%% and Fourier component of fundamental voltage=185.8V. For load 60 Ω, THD=1.07% and Fourier component of fundamental voltage=188V. For load, Load R=30 ohm and L=50mH, THD=3.29% and Fourier component of fundamental voltage=181V.

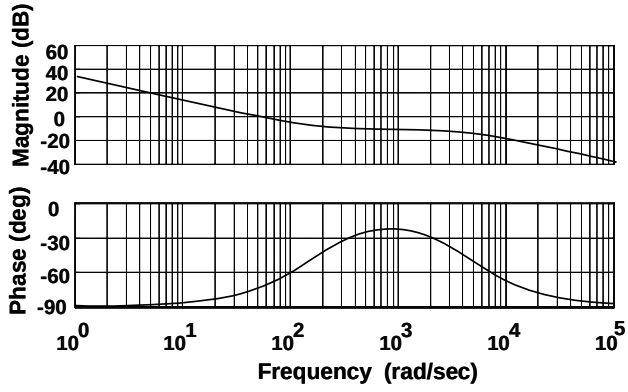

Fig. 18 Bode plot of T for the control block using FF-PWM

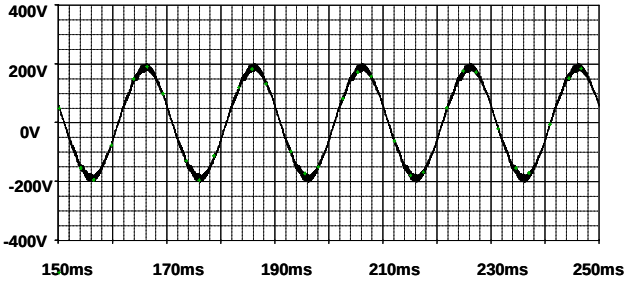

Fig. 19 Output voltage for load 30 Ω

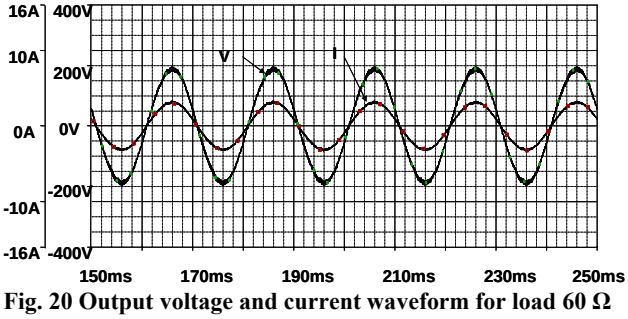

Fig. 20 Output voltage and current waveform for load 60 Ω

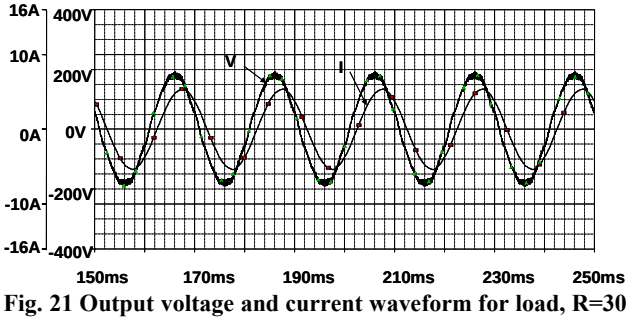

Fig. 21 Output voltage and current waveform for load, R=30 ohm and L=50mH.

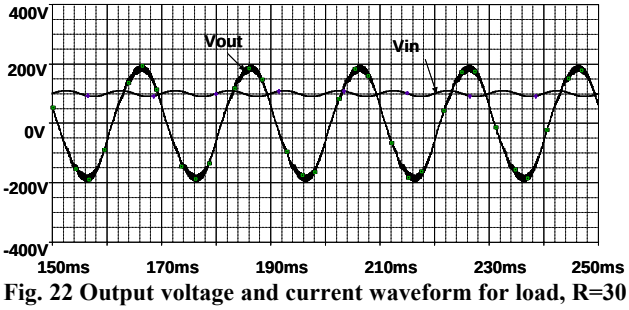

Fig. 22 Output voltage and current waveform for load, R=30 ohm and source voltage, Vin=100+10sin2ωt

For load 30 Ω, and Input voltage, Vg = Vin = 100 + 10 sin(2ωt), THD = 3.80% and Fourier component of fundamental voltage=186.2V. The controller works extremely well to regulate output voltage with source variation, inductive and resistive load variations as well as keeping THD within IEEE Std 519 i.e. THD<5%.

IV. Conclusion

This paper presents a simplified control strategy for the boost inverter with load and source variations. The method is based on feedforward compensation of source variation and voltage feedback technique using PI (proportional plus integral) compensator. It is shown that the resultant controller achieves the objective quite well. The results are tested by simulations. Future research can be done considering capacitive load and reduction of THD using second method. There is also scope to modify the conventional voltage mode controller considering inductive loads.

References

[1] Ram´on O. C´aceres and Ivo Barbi, "A Boost DC–AC Converter: Analysis, Design, and Experimentation," IEEE Transactions on Power Electronics, vol. 14, no. 1, pp. 134-141, January 1999.

[2] Vatche Vorperian, "Simplified Analysis of PWM Converters Using Model of PWM Switch Part I: Continuous Conduction Mode," IEEE Transactions on Aerospace and Electronic Systems, vol. 24, no. 3, pp. 490-496, May 1990.

[3] Khai D. T. Ngo, "Alternate Forms of the PWM Switch Models," IEEE Transactions on Aerospace and Electronic Systems, vol. 35, no. 4, pp. 1283-1292, October 1999.

[4] http://scholar.lib.vt.edu/theses/available/etd-11062000-08510043/unrestricted/Chapter2.pdf. From (DLA) Digital Library and Archives, Virginia Tech. DLA, 1989.

[5] Carolina Albea and Francisco Gordillo, "Control of the Boost DC-AC Converter with RL Load by Energy Shaping," Proceedings of the 46th IEEE Conference on Decision and Control, New Orleans, LA, USA, pp. 2417-2422, Dec. 12-14, 2007.

[6] Carolina Albea, Carlos Canudas-de-Wit and Francisco Gordillo, "Adaptive Control of the Boost DC-AC Converter," 16th IEEE International Conference on Control Applications Part of IEEE Multi-conference on Systems and Control Singapore, pp. 611-616, 1-3 October 2007.

[7] C Pablo Sanchis, Alfredo Ursæa, Eugenio Gubía and Luis Marroyo, "Boost DC–AC Inverter: A New Control Strategy," IEEE Transactions on Power Electronics, vol. 20, no. 2, pp. 343-353, March 2005.

[8] Barry Arbetter and Dragan Maksimovic, "Feedforward Pulse Width Modulators for Switching Power Converters," IEEE Transactions on Power Electronics, vol. 12, no. 2, pp. 361-368, March 1997.

[9] Ram´on O. C´aceres and Ivo Barbi, "A Boost DC–AC Converter: Operation, Analysis, and Experimentation," Proc. IEEE IECON'95 Conf., Orlando, FL, pp. 546-551, 5-11 November 1995.

[10] http://www.engr.colostate.edu/ECE562/lectures.html